

See discussions, stats, and author profiles for this publication at: <https://www.researchgate.net/publication/231739783>

Surface Modification of Au/TiO₂ Catalysts by SiO₂ via Atomic Layer Deposition

ARTICLE *in* THE JOURNAL OF PHYSICAL CHEMISTRY C · MAY 2008

Impact Factor: 4.77 · DOI: 10.1021/jp801484h

CITATIONS

56

READS

60

5 AUTHORS, INCLUDING:



Zhen Ma

Fudan University

98 PUBLICATIONS 2,204 CITATIONS

[SEE PROFILE](#)



Suree Brown

The University of Tennessee Medical Cente...

28 PUBLICATIONS 432 CITATIONS

[SEE PROFILE](#)



Jane Howe

Hitachi High-Technologies Canada Inc.

142 PUBLICATIONS 3,027 CITATIONS

[SEE PROFILE](#)

Surface Modification of Au/TiO₂ Catalysts by SiO₂ via Atomic Layer Deposition

Zhen Ma,[†] Suree Brown,[†] Jane Y. Howe,[‡] Steven H. Overbury,[†] and Sheng Dai*,[†]

Chemical Sciences Division and Materials Science and Technology Division, Oak Ridge National Laboratory, Oak Ridge, Tennessee 37831

Received: February 19, 2008; Revised Manuscript Received: April 1, 2008

Atomic layer deposition (ALD) was utilized for the surface engineering of metallic nanoparticles to tame their sintering problems and catalytic activities. We chose the surface modification of gold nanocatalysts as an example to demonstrate the concept of this ALD-based approach. Herein, an active Au/TiO₂ catalyst was modified by amorphous SiO₂ via ALD, and the samples were characterized by inductively coupled plasma-optical emission spectrometry (ICP-OES), scanning (SEM-EDX) and transmission electron microscope–energy-dispersive X-ray spectrometry (TEM-EDX), X-ray diffraction (XRD), and thermogravimetry/differential thermogravimetry (TG/DTG), and the catalytic activities in CO oxidation and H₂ oxidation were tested with respect to the pretreatment temperature and SiO₂ content. A significant sintering resistance and changes in catalytic activities were observed. The difference between the SiO₂/Au/TiO₂ samples prepared by gas-phase ALD and solution-phase chemical grafting was discussed.

1. Introduction

Supported metal catalysts (e.g., Pt/Al₂O₃) usually contain simple metal–support interfaces. Evidence exists for the migration of part of a reducible metal oxide support (e.g., TiO₂) onto a group VIII metal (e.g., Pt) under H₂ at elevated temperatures.^{1–5} This unique feature of strong metal–support interaction (SMSI) has inspired the construction of artificial catalytic architectures with complex interfacial structures. For instance, Bell and co-workers found that the adsorption of H₂ and CO on TiO₂-modified Rh/SiO₂ and Pd/SiO₂ was suppressed.^{3,6} Horváth and co-workers reported that TiO₂-decorated Au/SiO₂ was more active than Au/SiO₂ in CO oxidation because of the creation of an active Au–TiO₂ interface.⁷ The coating of Pt/zeolite and Pt/C by a SiO₂ matrix could suppress the sintering of Pt nanoparticles for three-way catalysis and electrocatalysis, respectively.^{8,9} CdS-coated Au/TiO₂ and Cr₂O₃-coated Rh/(Ga_{1-x}Zn_x)(N_{1-x}O_x) exhibited superior performance in photocatalysis.^{10,11} These catalysts all possess unique metal–modifier and modifier–support interfaces in addition to the conventional metal–support interface. It would be interesting to develop versatile methodologies for the construction of analogous architectures and to search for structure–function correlations.

Atomic layer deposition (ALD) is a self-limiting and sequential surface modification technique that allows for the conformal coating on flat and powder surfaces.^{12–15} Our group has successfully demonstrated its applications in the fine-tuning of the pore size of mesoporous SiO₂ as well as in the surface functionalization of silver island films for surface-enhanced Raman spectroscopy.^{16,17} Although ALD has received significant enthusiasm among the materials community, it has been less commonly employed in catalysis to deposit metal particles on supports^{18,19} and to modify supports by other metal oxides.^{20–23} Notably, Pellin et al. and Stair et al. coated nanostructured membranes by V₂O₅ via ALD, and demonstrated their superior selectivity in oxidative dehydration of cyclohexane.^{21,23} Nev-

ertheless, virtually no attempt has been made in the literature to post-modify supported metal catalysts via ALD. To the best of our knowledge, the only noticeable example distantly related to the current context is that in which Fan and co-workers utilized gold nanoparticles to catalyze the growth of ZnO nanowires, and then coated the Au–ZnO composite by Al₂O₃ thin films via ALD.²⁴ The Al₂O₃@Au–ZnO material transformed into ZnAl₂O₄ spinel nanotubes upon annealing due to the Kirkendall effect, but the applications of this material were not reported. Below we present a case on the post modification of supported gold catalysts via ALD.

Catalysis by gold nanoparticles has attracted much attention recently.^{25–29} Supported gold catalysts are usually prepared by loading gold onto single-component supports.³⁰ To explore the subtle effects of catalyst preparation and structure on catalytic performance, more complex catalytic structures may be constructed.^{7,31–42} Our group recently reported that the post-modification of Au/TiO₂ by SiO₂ using a solution-phase chemical grafting method could stabilize gold nanoparticles and maintain high activity in CO oxidation after treating the SiO₂/Au/TiO₂ sample in O₂–He at 700 °C.⁴¹ Herein, we employ an alternative gas-phase ALD method for the fabrication of SiO₂/Au/TiO₂ catalysts (Figure 1), and report on their characterization data and catalytic performance. The objective of this work is to demonstrate the feasibility of using ALD to generate novel metal–modifier and modifier–support interactions based on Au/TiO₂ and to explore the subtle effects of catalyst preparation and interfacial structure on catalytic performance. The resulting surface morphology is reminiscent of the metal oxide-encapsulated metal nanoparticles generated via SMSI on reducible metal oxide supports.^{43,44} One of the key features of our current methodology for deriving oxide-encapsulated metallic nanoparticles is that it is not necessary to rely on reducible metal oxide supports for invoking surface restructuring under reducing atmosphere. Nonreducible oxides (e.g., SiO₂) can also be employed to construct SMSI-like interfaces. To the best of our knowledge, the migration of part of reducible support (e.g., TiO₂) onto gold nanoparticles via the SMSI effect has not been observed so far.⁴⁵ Therefore, the ALD-based approach described

* Corresponding author. E-mail: dais@ornl.gov. Tel: 1-865-576-7307. Fax: 1-865-576-5235.

[†] Chemical Sciences Division.

[‡] Materials Science and Technology Division.

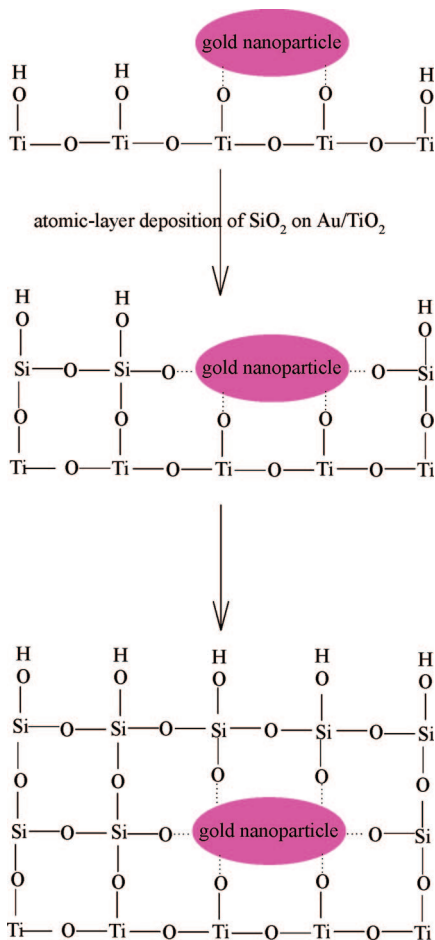


Figure 1. Schematic representation for the ALD of amorphous SiO₂ onto Au/TiO₂.

in the current work may open up a new avenue for the construction of versatile model catalysts with complex metal–support, metal–modifier, and modifier–support interfaces.

2. Experimental Section

Au/TiO₂ was prepared by deposition–precipitation.^{25–29} A solution containing 0.6 g HAuCl₄·3H₂O in water (100 mL) was adjusted to pH 10.0 using 1.0 M KOH. The resulting solution was heated at 80 °C, 2.0 g of TiO₂ (Degussa P25) was added, and the slurry was magnetically stirred for 2 h. The precipitate was centrifuged and washed four times with water. In each washing–centrifugation cycle, the solid deposited at the bottom of the centrifuge tube was redispersed using a vortexer, and then recentrifuged. The product was dried at 40 °C for 2 days. Several batches of Au/TiO₂ were synthesized in parallel, ground into fine powders, homogeneously mixed into one container, and calcined in a muffle oven at 250 °C for 2 h. The gold content was measured by inductively coupled plasma-optical emission spectrometry (ICP-OES) as 2.3 wt %.

ALD experiments were carried out in a rotary evaporator connected to a homemade ALD reactor.⁴⁶ Electronically controlled two-way solenoid valves, with 3-mm orifices, were used to accurately time the exposures. During the reaction, the powder substrate (i.e., 300–450 mg of 250 °C-calcined Au/TiO₂) was exposed evenly to precursors by being rotated at a high speed in a rotary evaporator. Tetramethyl orthosilicate (TMOS) and water vapor were alternatively introduced into the reaction flask under vacuum (10–20 mTorr) and at a reaction temperature of 150 °C. Each ALD cycle consisted of the following steps: (1)

exposure to TMOS, 5 min; (2) removal of unreacted TMOS under vacuum, 4 min; (3) exposure to water vapor, 5 min; and (4) removal of unreacted water vapor under vacuum, 3 min. SiO₂/Au/TiO₂ samples with Si/Ti ratios of 0.06 and 0.11 were prepared after 15 and 25 cycles, respectively. These samples, without subsequent thermal pretreatment at elevated temperatures in the catalytic reactor, are referred to “as-prepared” SiO₂/Au/TiO₂.

CO oxidation was tested in a plug-flow microreactor (Altamira AMI 200). A catalyst sample (50 mg) was loaded into a U-shaped quartz tube (4 mm i.d.), and pretreated in flowing 5% O₂ (balance He) at a specified temperature for 1 h. The catalyst was cooled down, the gas stream switched to 1% CO in dry air (flow rate of 37 cm³/min) and the reaction temperature ramped using a furnace or by immersing the U-shaped tube in ice–water or acetone–liquid nitrogen to record the light-off curve. A portion of the product stream was extracted periodically with an automatic sampling valve, and analyzed using a dual-column gas chromatograph with a thermal conductivity detector. The CO conversion was calculated as $X_{CO} = [CO_2]_{out}/[CO]_{out} + [CO_2]_{out}$, where [CO₂]_{out} and [CO]_{out} refer to the concentrations of CO₂ and CO exiting the reactor, respectively.

Catalytic H₂ oxidation was tested in the same plug-flow microreactor following the pretreatment procedure described above. During the reaction, 50 cm³/min of 5% O₂ (balance He) and 5 cm³/min of pure H₂ were mixed and passed through the catalyst bed containing 50 mg of catalyst, and the reaction temperature was ramped using a furnace. The H₂ conversion was calculated as $X_{H_2} = ([H_2]_{in} - [H_2]_{out})/[H_2]_{in}$, where [H₂]_{in} refers to the average H₂ concentration in blank tests where 50 cm³/min of 5% O₂ (balance He) and 5 cm³/min of pure H₂ were passed through a U-type tube without catalyst at room temperature.

X-ray diffraction (XRD) data were collected on a Siemens D5005 diffractometer with Cu K α radiation. The average gold particle sizes were estimated from X-ray line broadening analysis applying the Debye–Scherrer equation on the (220) diffraction ($2\theta = 44^\circ$) of gold. Gold content was measured using ICP-OES on a Thermo IRIS Intrepid II spectrometer. The Si/Timolarratio was estimated by scanning electron microscope–energy-dispersive X-ray spectrometry (SEM-EDX) on a JEOL JSM-6060 SEM coupled with an EDX detector. The transmission electron microscope (TEM) experiments reported in Figures 2 and 3 were carried out on a Hitachi HF-2000 TEM at 200 kV. The samples were dusted onto a lacey carbon film coated 300-mesh copper grid. The TEM or TEM-EDX experiments reported in Figures 4, 9, 10, S1, and S2 were carried out using a Hitachi HF-3300 cold-field emission TEM/STEM coupled with a Thermo-Noran EDX analyzer. Thermogravimetry/differential thermogravimetry (TG/DTG) experiments were conducted on a TGA 2950 instrument using a heating rate of 10°/min under air atmosphere.

3. Results

3.1. TEM and EDX characterization of as-synthesized SiO₂/Au/TiO₂ samples. Figure 2A shows a TEM image of as-synthesized SiO₂/Au/TiO₂ (Si/Ti = 0.06) prepared by the modification of 250 °C-calcined Au/TiO₂ with SiO₂ via ALD. No subsequent pretreatment or reaction testing was conducted before recording the TEM image of this as-synthesized SiO₂/Au/TiO₂ sample. Gold nanoparticles, with sizes below 5 nm in the majority of the cases, were homogeneously distributed on TiO₂ (Degussa P25) crystallites with grain sizes of 20–50 nm.

A high-resolution TEM image of as-synthesized SiO₂/Au/TiO₂ (Si/Ti = 0.06) is shown in Figure 2B. Amorphous SiO₂

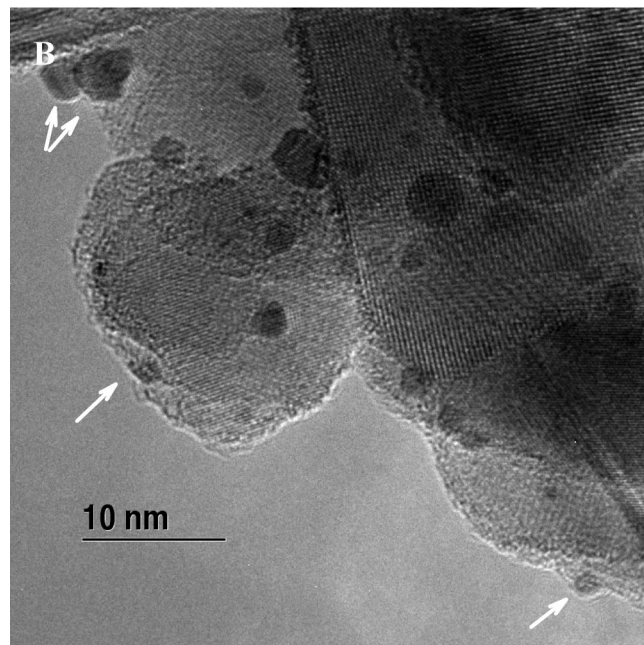
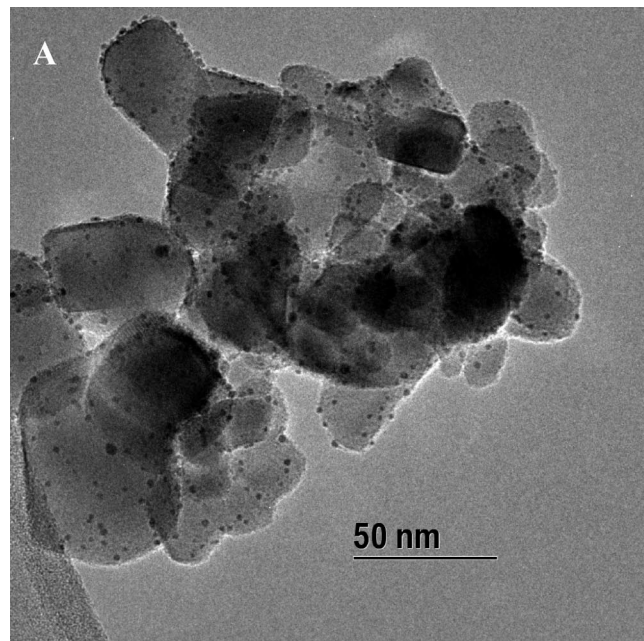


Figure 2. TEM images of as-synthesized Si₂/Au/TiO₂ (Si/Ti = 0.06) catalyst without undergoing thermal pretreatment and reaction testing.

decoration or coating may not be seen easily with top views where electron beams pass through both gold nanoparticles and the underlying TiO₂ support, but it is more easily detected from side views,⁴³ where the image shows that gold nanoparticles were either partially modified or encapsulated by amorphous SiO₂. The white arrows in Figure 2B point to the interfacial structures from side views. A survey of TEM images like this indicated that in the majority of cases gold nanoparticles were partially modified, but not completely encapsulated, by amorphous SiO₂.

Figure 3 shows representative TEM images of as-synthesized Si₂/Au/TiO₂ with more SiO₂ content (Si/Ti = 0.11). Again, for those gold particles on TiO₂ and the electron beam passing through both gold and TiO₂, the SiO₂ coating cannot be easily resolved, and the scenarios are clearer with side views (pointed

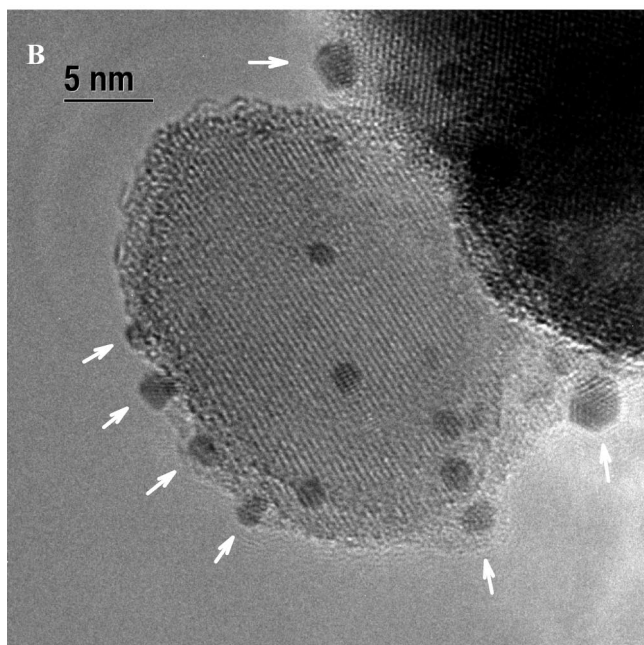
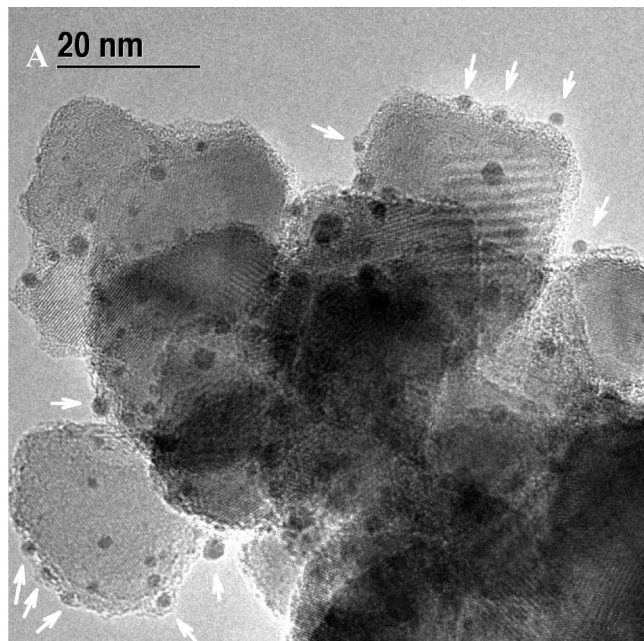


Figure 3. TEM images of as-synthesized Si₂/Au/TiO₂ (Si/Ti = 0.11) catalyst without undergoing thermal pretreatment and reaction testing.

out by white arrows). This time, with more SiO₂ uptake, the capping of gold nanoparticles and the support was more obvious. Some gold nanoparticles were encapsulated by amorphous SiO₂ matrix, while others were only partially modified. The general surface morphology appears to resemble the oxide encapsulation of metallic nanoparticles supported on reducible metal oxide supports, which is induced by the SMSI under H₂ atmosphere. For example, similar morphologies of metal oxide-capped metal particles were seen in the TEM images of Pd/TiO₂ (Figure 18.6 in reference 43) and Rh/La₂O₃ (Figure 19.11 in reference 44) reduced in H₂ at high temperature. Nevertheless, in those cases, the formation of TiO_x and La₂O_x coatings was due to the SMSI mechanism, which is apparently different from the case reported here, if we adopt the textbook definition of SMSI.^{47,48} The fact that the analogous interfacial structures can be generated via

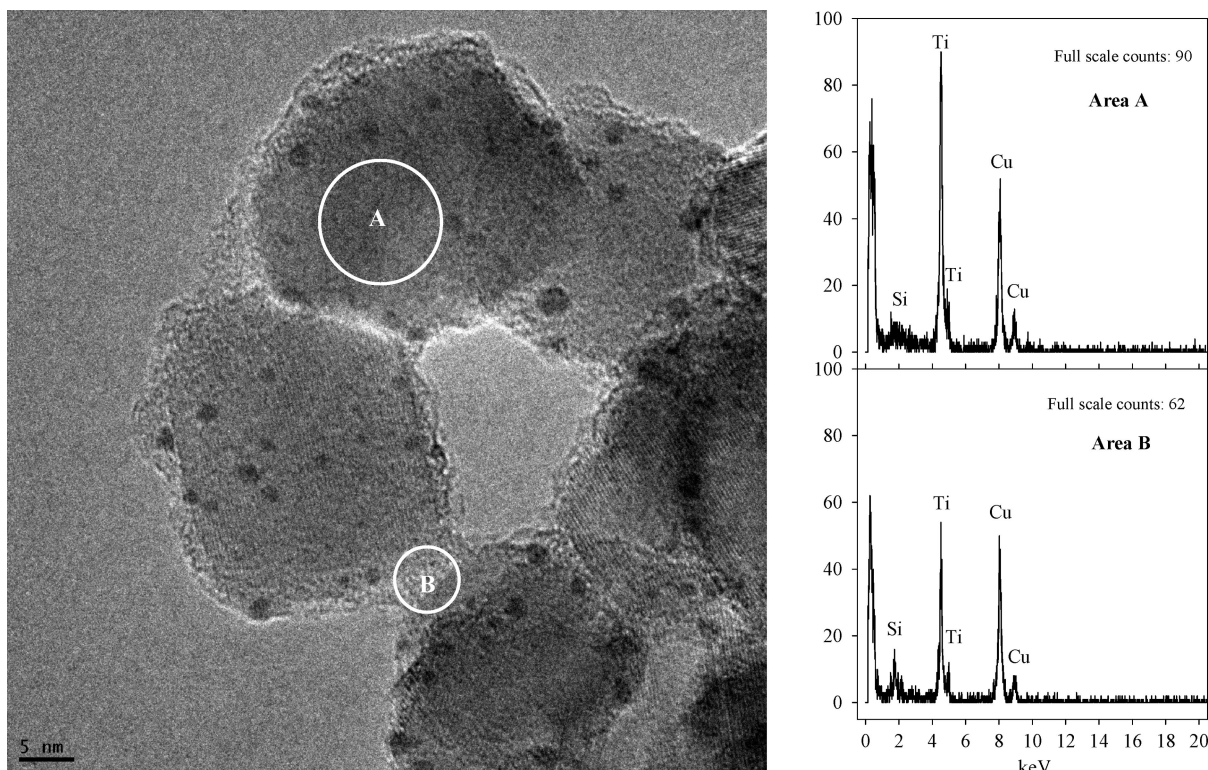


Figure 4. A TEM image of as-synthesized SiO₂/Au/TiO₂ (Si/Ti = 0.11) catalyst and selected-area EDX results.

ALD with a nonreducible oxide is interesting, considering that only reducible oxide supports can be used in the SMSI scenario to cover metal nanoparticles.¹

The TiO₂ support was also coated by SiO₂, as seen from TEM images (e.g., Figure 3). To confirm the identity of the amorphous coatings, we conducted selected-area EDX experiments, and detected Si element on TiO₂ surfaces (Figure 4). Specifically, the EDX spectra in Figure 4 correspond to area A at the center of a TiO₂ crystal surface and area B at the bridging edges of two TiO₂ crystals. Because the electron beam goes through the entire thickness of the material, the Si/Ti ratio is higher at the edge (area B) than that of the center (area A), suggesting that the observed outer thin layer is SiO₂ coating.

3.2. Catalytic Performance and Relevant XRD Characterization. The performance of SiO₂/Au/TiO₂ in CO oxidation was compared with that of Au/TiO₂. Au/TiO₂ was synthesized by deposition-precipitation, and calcined in a muffle oven at 250 °C. It was then either tested as such or pretreated in O₂–He at 300–700 °C prior to the reaction testing. As shown in Figure 5A, 250 °C-calcined Au/TiO₂ was very active for CO oxidation, achieving 50% CO conversion at –41 °C and complete conversion at –25 °C. The activity of Au/TiO₂ decreased significantly upon thermal treatment: the T_{50} (temperature required for 50% conversion) values increased to 17, 115, and 142 °C when Au/TiO₂ was pretreated at 300, 500, and 700 °C, respectively.

Figure 5B summarizes the XRD patterns of Au/TiO₂ collected after the pretreatment at different temperatures and subsequent reaction testing. Gold ($2\theta = 38, 44, 65, 78$, and 82°)^{49,50} and TiO₂ (anatase and rutile) peaks were identified for these samples. The gold peaks generally increased with the pretreatment temperature (for a quick reference, compare the sharpness of the gold peak at $2\theta = 44^\circ$: the sharper the gold peaks, the bigger the gold particles). The average gold particle sizes of Au/TiO₂ calcined or pretreated at 250, 300, 500, and 700 °C were 4.7, 4.7, 9.4, and 17.0 nm, respectively, as estimated by the XRD analysis.

analysis. The increase of gold particle sizes with the pretreatment temperature may explain the decrease in activity of Au/TiO₂ upon thermal treatment.

Figure 6A shows the catalytic performance of SiO₂/Au/TiO₂ (Si/Ti = 0.06) in CO oxidation. Compared with 250 °C-calcined Au/TiO₂ (Figure 5A), as-synthesized SiO₂/Au/TiO₂ was not particularly active for CO oxidation, achieving T_{50} at 112 °C, compared to the –41 °C value for uncoated Au/TiO₂. Pretreating SiO₂/Au/TiO₂ in O₂–He at 300 °C somewhat increased the activity when the reaction temperature was below 100 °C, probably because the pretreatment at 300 °C may remove organic moieties originating from the TMOS precursor.⁴¹ A slight weight loss (0.2 wt%) of the catalyst in the range of 200–350 °C was detected by TG/DTG (data not shown). It is generally recognized that organic fragment-passivated metal surfaces are less active than clean metal surfaces.^{51,52} Back to Figure 6A, another observation is that the activities of SiO₂/Au/TiO₂ pretreated at different temperatures were comparable at higher reaction temperatures.

Figure 6B summarizes the XRD patterns of SiO₂/Au/TiO₂ (Si/Ti = 0.06) collected after the pretreatment at different temperatures and subsequent reaction testing. The gold peaks increased with the pretreatment temperature, but the extent of the increase was not very obvious compared with the extent observed in Figure 5B. The average gold particle sizes of as-synthesized, 300 °C-pretreated, 500 °C-pretreated, and 700 °C-pretreated SiO₂/Au/TiO₂ catalysts were 4.7, 4.8, 6.1, and 8.5 nm, respectively, as estimated by the XRD analysis. Obviously, the modification of Au/TiO₂ by SiO₂ could stabilize gold nanoparticles against sintering.

Figure 7 shows the CO conversions on as-synthesized and 700 °C-pretreated SiO₂/Au/TiO₂ (Si/Ti = 0.11) as well as the XRD patterns of the catalysts collected after the pretreatment and subsequent reaction testing. This time, with more SiO₂ content, the gold nanoparticles were protected by SiO₂ matrix more obviously (Figure 3), and the gold particle sizes were

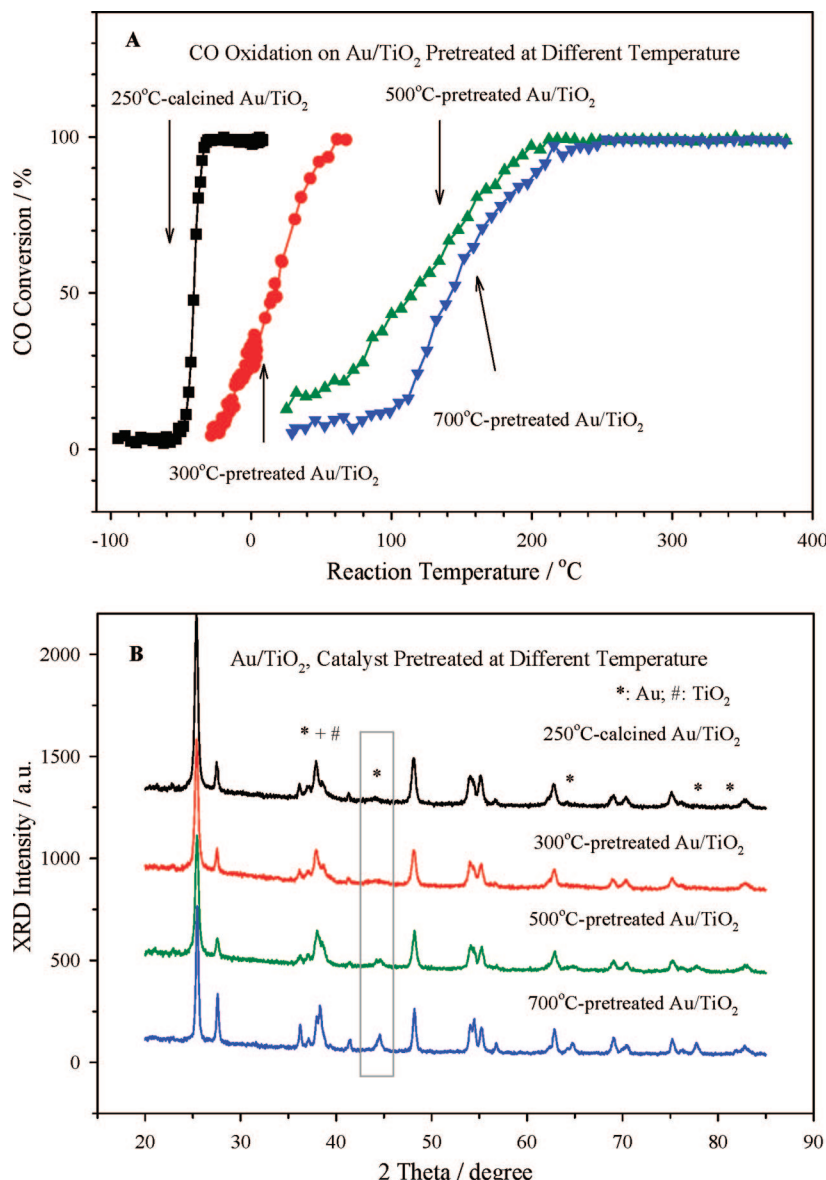


Figure 5. Top: CO conversions on Au/TiO₂ pretreated at different temperature. Bottom: XRD patterns of Au/TiO₂ samples collected after the pretreatment at different temperatures and reaction testing.

maintained after 700 °C-pretreatment to a greater extent (5.8 nm, as estimated by the XRD data in Figure 7B). Nevertheless, the activities of SiO₂/Au/TiO₂ (Si/Ti = 0.11, Figure 7A) in CO oxidation were even lower than those of Au/TiO₂ (Figure 5A) and SiO₂/Au/TiO₂ (Si/Ti = 0.06, Figure 6A). Apparently, the stabilization of gold nanoparticles by SiO₂ additives did not guarantee high activity in CO oxidation, and the active sites were partially covered by the SiO₂ matrix.

Figure 8 compares the performance of Au/TiO₂ and SiO₂/Au/TiO₂ (Si/Ti = 0.06) in H₂ oxidation. The 250 °C-calcined Au/TiO₂ was active for H₂ oxidation, achieving complete H₂ conversion below 80 °C. The activity of Au/TiO₂ in H₂ oxidation obviously decreased as the pretreatment temperature was increased. The sharp decrease of activity in H₂ oxidation may be explained by the obvious sintering of gold nanoparticles as well. Comparing the CO conversion and H₂ conversion on the same Au/TiO₂ pretreated under different temperatures (Figure 5A versus Figure 8A), it seems that the reactivity of CO is generally higher than that of H₂, and such difference as a function of pretreatment temperature (and gold particle size)

may be employed in the future for designing selective catalysts for CO oxidation in the presence of H₂.

In contrast, Figure 8 also shows that the as-synthesized SiO₂/Au/TiO₂ (Si/Ti = 0.06) was less active in H₂ oxidation than 250 °C-calcined Au/TiO₂, achieving complete H₂ oxidation at 120 °C (compared with 80 °C for 250 °C-calcined Au/TiO₂). The lower activity in H₂ oxidation is again consistent with the coverage of gold nanoparticles by SiO₂. The pretreating of SiO₂/Au/TiO₂ in O₂-He at 300 °C somewhat increased the activity, again possibly because of the removal of residual organic moieties derived from the TMOS precursor. As described earlier, a slight weight loss (0.2 wt%) of the catalyst in the range of 200–350 °C was detected by preliminary TG/DTG experiments. The further high-temperature pretreatment of SiO₂/Au/TiO₂ decreased the activity in H₂ oxidation, although the activity was still higher than Au/TiO₂ pretreated at the corresponding temperatures. This could be due to the fact that, the sintering of gold nanoparticles on SiO₂/Au/TiO₂ was not as severe as that on Au/TiO₂. Interestingly, the reactivity of H₂ on SiO₂/Au/TiO₂

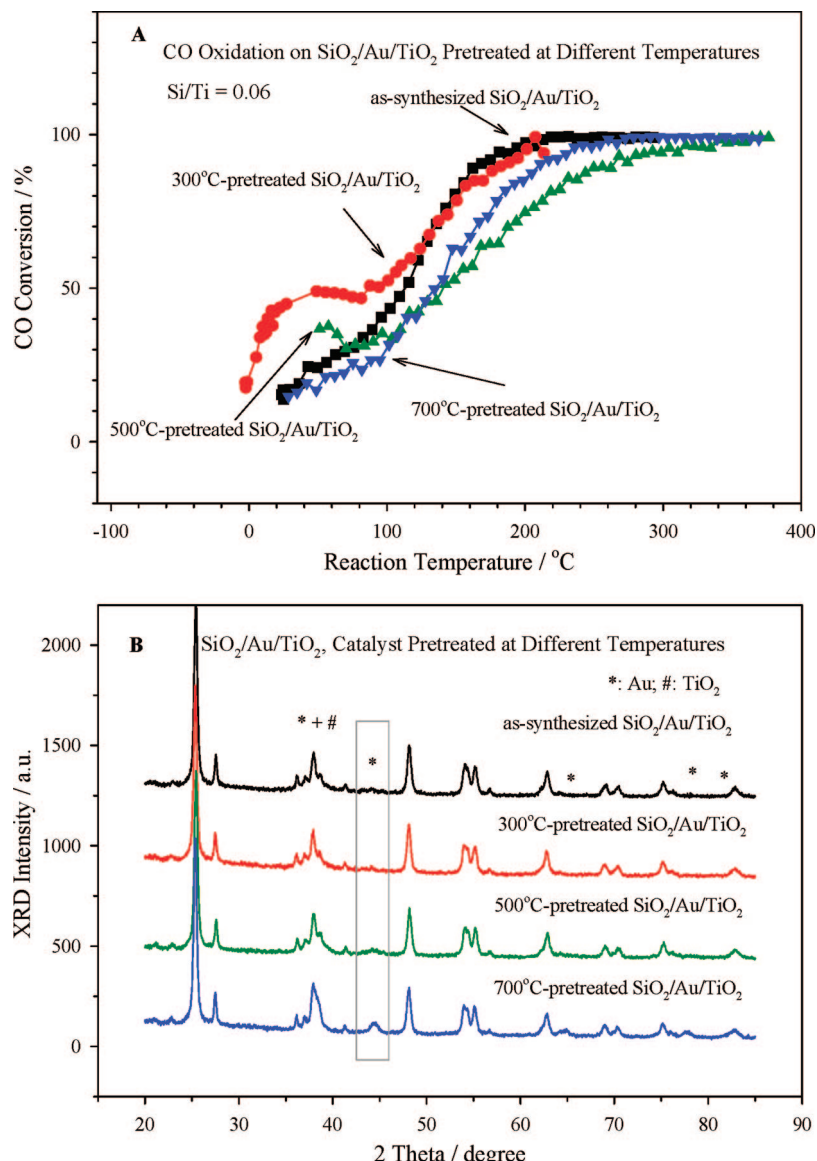


Figure 6. Top: CO conversions on SiO₂/Au/TiO₂ (Si/Ti = 0.06) pretreated at different temperatures. Bottom: XRD patterns of SiO₂/Au/TiO₂ (Si/Ti = 0.06) samples collected after the pretreatment at different temperatures and reaction testing.

decreased significantly upon increasing the pretreatment temperature (Figure 8B), whereas the CO light-off curves of the sample clustered together (Figure 6A). This implies that H₂ oxidation and CO oxidation may not follow the same mechanism or may require different active sites. Overall, our data show that via surface modification of Au/TiO₂ by SiO₂, it is possible to tune the reactivity of H₂ oxidation and CO oxidation. This feature may be very useful in the selective oxidation of CO or H₂ in CO + H₂ + O₂ streams.

3.3. TEM Characterization of SiO₂/Au/TiO₂ Catalysts Collected after CO Oxidation. In Section 3.1, we reported the TEM images of as-synthesized SiO₂/Au/TiO₂ samples (Si/Ti = 0.06 and 0.11, respectively) without undergoing thermal pretreatment and reaction testing. Nevertheless, one question arises as to whether the SiO₂ decoration or coating remains after the thermal pretreatment and catalytic reaction. This question is valid because, if all the gold nanoparticles were completely encapsulated in the SiO₂ matrix with no breakage of the SiO₂ shells, the XRD peaks corresponding to metallic gold should not become sharper with the pretreatment temperature (Figures 6B and 7B). To investigate this question, we selected SiO₂/Au/

TiO₂ (Si/Ti = 0.11) samples collected after the reaction testing depicted in Figure 7A for TEM surveys.

The TEM images in Figure 9 correspond to the used SiO₂/Au/TiO₂ (Si/Ti = 0.11) collected after testing the as-synthesized catalyst, whereas those in Figure 10 correspond to the used catalyst collected after the pretreatment in O₂–H₂ at 700 °C and subsequent reaction testing reported in Figure 7. As shown by these representative images, in many cases smaller gold nanoparticles were still coated by the SiO₂ matrix, whereas bigger gold nanoparticles were either not coated or the coating was too thin to be unambiguously distinguished. Figures S1 and S2 in the Supporting Information provide more images of these samples. It is speculated that some uncoated or not-well-coated gold nanoparticles in the as-synthesized SiO₂/Au/TiO₂ may migrate during the thermal treatment to form bigger gold particles, whereas the densely coated gold nanoparticles may remain intact.

4. Discussion

In this work, we have successfully constructed additional artificial metal-modifier (Au-SiO₂) and modifier-support

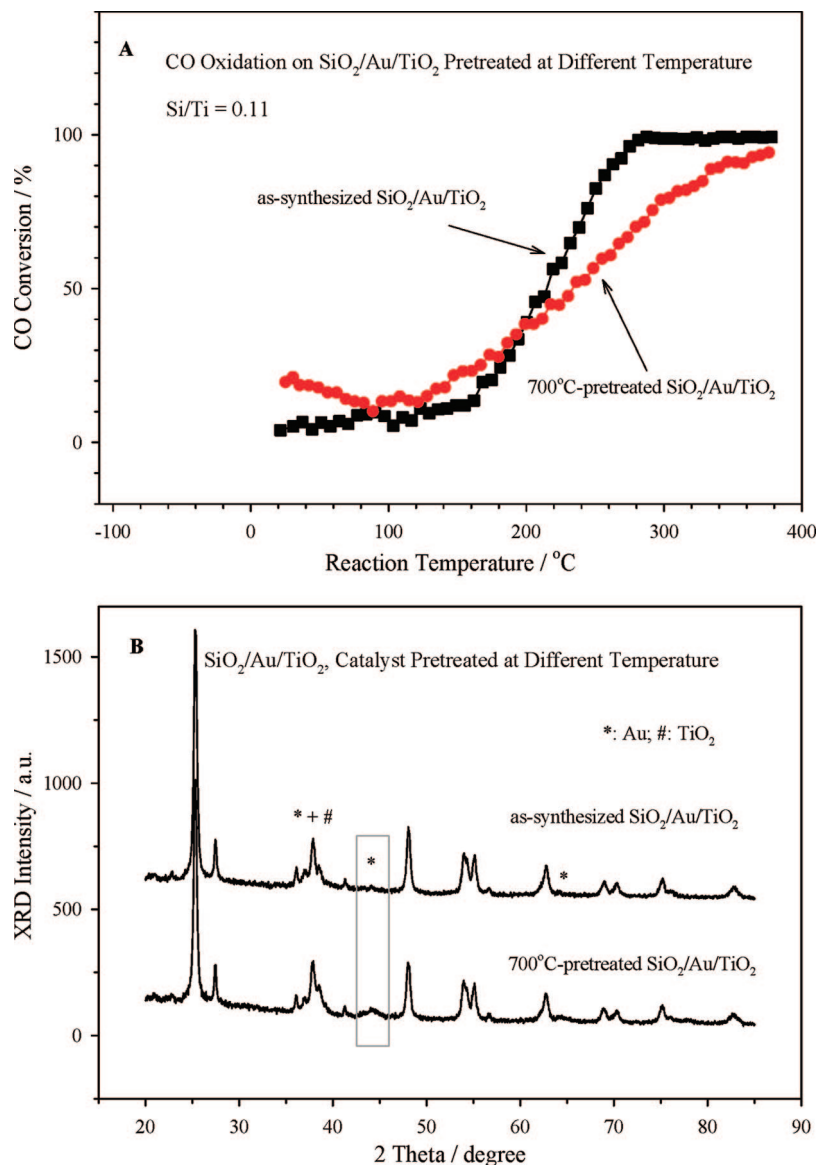


Figure 7. Top: CO conversions on $\text{SiO}_2/\text{Au}/\text{TiO}_2$ ($\text{Si}/\text{Ti} = 0.11$) pretreated at different temperatures. Bottom: XRD patterns of $\text{SiO}_2/\text{Au}/\text{TiO}_2$ ($\text{Si}/\text{Ti} = 0.11$) samples collected after the pretreatment at different temperatures and reaction testing.

($\text{SiO}_2-\text{TiO}_2$) interfaces by modifying Au/TiO_2 catalysts by amorphous SiO_2 via ALD. Comparing $\text{SiO}_2/\text{Au}/\text{TiO}_2$ prepared by solution-phase chemical grafting⁴¹ and gas-phase ALD, it is generalized that the SiO_2 in both cases could stabilize gold nanoparticles. This stabilizing effect is dependent on the SiO_2 content, being more obvious when gold nanoparticles are encapsulated in the SiO_2 matrix (the TEM image in Figure 3 and XRD data in 7B for $\text{SiO}_2/\text{Au}/\text{TiO}_2$ with Si/Ti ratio of 0.11). Similarly, Kanazawa impregnated Pt/zeolite with $\text{Si(OCH}_3)_4$, and found that Pt nanoparticles were still small even after calcination at 800 °C.⁸ Tsang and co-workers coated Pt colloids by amorphous SiO_2 using a microemulsion method, and then dispersed the Pt@ SiO_2 core–shell structure onto a support.^{53,54} They found that the SiO_2 coating could stabilize Pt nanoparticles against sintering. Collectively, these data indicate that the coating of metal nanoparticles by SiO_2 can indeed stabilize metal nanoparticles. Such thermal stability is very desirable in catalysis because the sintering of metal nanoparticles is a key issue there.

Conceptually, small gold particles may lead to high activity in CO oxidation,^{25–29} but the stabilization of gold nanoparticles in $\text{SiO}_2/\text{Au}/\text{TiO}_2$ does not necessarily guarantee high activity.

While $\text{SiO}_2/\text{Au}/\text{TiO}_2$ catalysts prepared by liquid-phase chemical grafting in our previous publication were still active after high-temperature treatment,⁴¹ those prepared by gas-phase ALD in our current work were not particularly active, even though the gold particles were small in certain cases (e.g., low pretreatment temperature, high SiO_2 loading). This difference points to another effect of SiO_2 . Namely, SiO_2 coats or partially modifies the TiO_2 support, gold nanoparticles, and the interface between gold and TiO_2 , thus blocking the active sites and reducing the activity. In the literature, amorphous TiO_2 decoration on group VIII metals strongly suppressed the adsorption of CO and H_2 , and diminished the activity in hydrogenolysis.¹ Oyama and co-workers modified Al_2O_3 support by chemical vapor deposition of $\text{Si(OC}_2\text{H}_5)_4$ at 600 °C, and found that the thick SiO_2 film (20–30 nm) significantly deterred the passage of CH_4 , CO, and CO_2 through the $\text{SiO}_2/\text{Al}_2\text{O}_3$ membrane.⁵⁵

The net catalytic result of $\text{SiO}_2/\text{Au}/\text{TiO}_2$ may be a compromise between these two counteracting effects of the SiO_2 additive, and these effects (the stabilization of the gold nanoparticles and the inhibition of the catalytic activity) are related to preparation methods and preparation details. In our previous

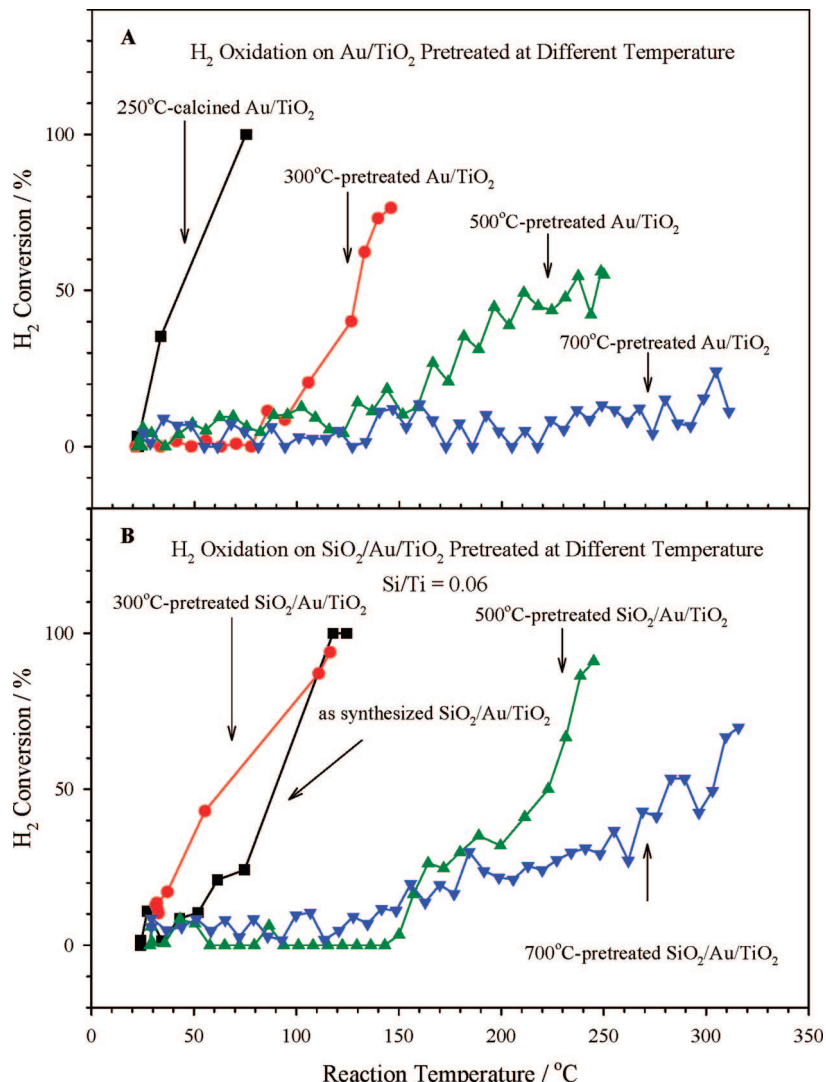


Figure 8. Top: H₂ conversions on Au/TiO₂ pretreated at different temperatures. Bottom: H₂ conversions on SiO₂/Au/TiO₂ (Si/Ti = 0.06) pretreated at different temperatures.

publication,⁴¹ SiO₂/Au/TiO₂ samples were prepared by solution-phase chemical grafting, and no water was added to hydrolyze the anchored Si(OCH₃)₄. The pretreatment of as-synthesized SiO₂/Au/TiO₂ in O₂–He at elevated temperatures removed the organic fragments and entrapped organic solvent molecules, leaving behind porous SiO₂ surface structures that not only stabilized gold nanoparticles but also maintained the activity.⁴¹ We notice that SiO₂/Pt/zeolite⁸ and supported Pt@SiO₂^{53,54} prepared using traditional solution-based methods also showed high activity in CO oxidation,⁸ NO_x reduction,⁸ C₃H₆ combustion,⁸ *n*-butane combustion,⁵³ and toluene hydrogenation⁵⁴ after high-temperature calcination, implying that SiO₂ coatings synthesized via these solution-based methods did not significantly block the active sites. The porosity of these SiO₂ coatings may result from the thermal removal of entrapped organic moieties and solvent molecules that function as porogens.⁵⁶

Nevertheless, for the ALD-based methodology reported here, water vapor was supplied during each ALD cycle to hydrolyze the Si–OCH₃ groups, and a vacuum was used to remove organic fragments more sufficiently. We conducted TG/DTG experiments, which indicated that the weight loss of SiO₂/Au/TiO₂ (Si/Ti = 0.11) synthesized via ALD was 0.4 wt % in the range of 200–350 °C. This weight loss is much smaller than the 3.5 wt % value corresponding to SiO₂/Au/TiO₂ (Si/Ti = 0.10)

synthesized via liquid-phase grafting in our previous publication.⁴¹ Therefore, the SiO₂ layers introduced by ALD might have a more dense surface structure considerably passivating some active sites, although SiO₂ did stabilize gold particles. Therefore, to tune the activity and selectivity of this type of SiO₂/Au/TiO₂ catalysts, one may want to cope with the two counteracting effects of SiO₂ in order to get the desired functionality. Different synthesis methods and synthesis details play an important role in this activity and selectivity manipulating.

In our current scenario, we have shown that the reactivities in CO oxidation and H₂ oxidation were changed as a result of the surface modification of Au/TiO₂ by SiO₂ (Figures 5–7). This reactivity change is summarized in Figure S3 of the Supporting Information. It can be seen in Figure S3 that the activity of SiO₂/Au/TiO₂ (Si/Ti = 0.06) in CO oxidation was generally higher than that of Au/TiO₂, and the reactivity was comparable only when both SiO₂/Au/TiO₂ (Si/Ti = 0.06) and Au/TiO₂ were pretreated at 700 °C. On the other hand, the activity of SiO₂/Au/TiO₂ (Si/Ti = 0.06) in H₂ oxidation was generally higher than that of Au/TiO₂, except when SiO₂/Au/TiO₂ was not pretreated to remove a small amount of residual organic moieties. As seen clearly from Figure S3, the reactivities toward CO oxidation versus H₂ oxidation could be adjusted in different degrees by modifying Au/TiO₂ with SiO₂ and by changing the

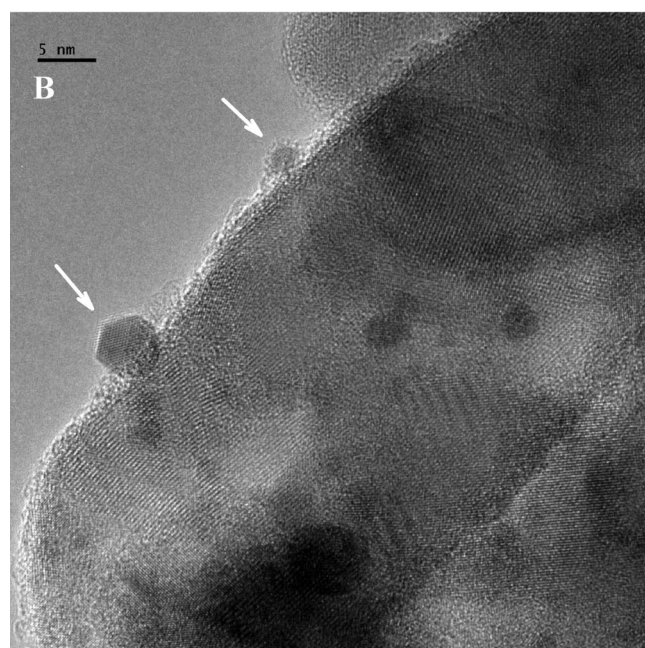
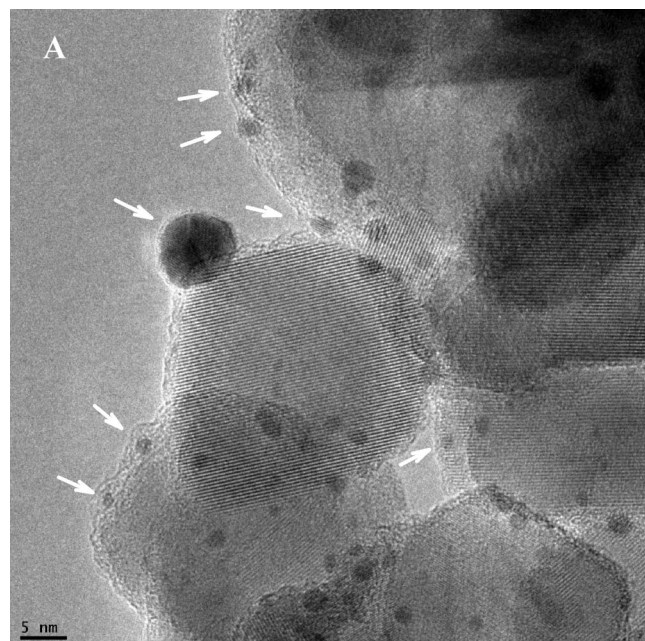


Figure 9. TEM images of used $\text{SiO}_2/\text{Au}/\text{TiO}_2$ ($\text{Si}/\text{Ti} = 0.11$) collected after testing the as-synthesized sample in CO oxidation without thermal pretreatment.

pretreatment temperatures. Such changes in reactivity preference are potentially useful for tuning the selectivity in catalysis.

5. Conclusions

Conventional metal catalysts have simple metal–support interfaces. In this work, we successfully introduced additional metal–modifier and modifier–support interfaces by modifying Au/TiO_2 catalysts by amorphous SiO_2 via ALD. The presence of SiO_2 decoration on gold nanoparticle surfaces and on the support surfaces was confirmed by TEM-EDX, the thickness of which increased with the SiO_2 content. The interfacial structure is reminiscent of the metal oxide-encapsulated metal nanoparticles generated via SMSI on reduced metal oxide supports. The presence of SiO_2 stabilized gold nanoparticles against sintering, and it also tuned the activities of the catalysts

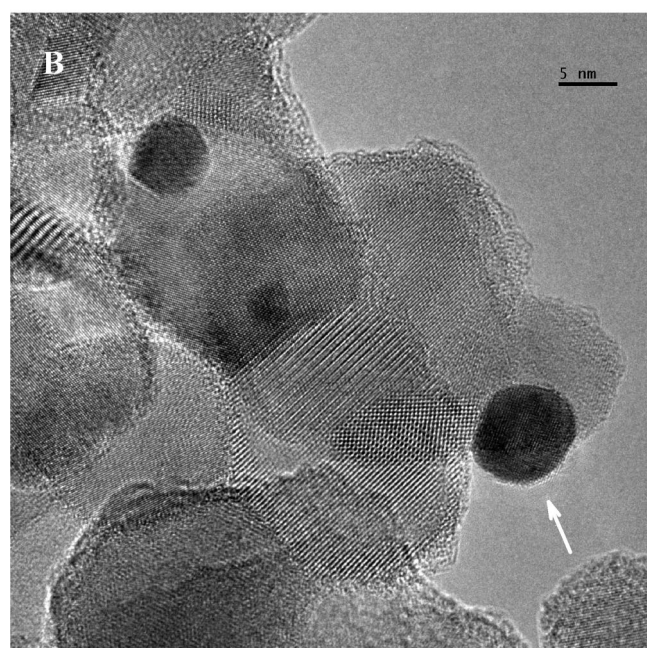
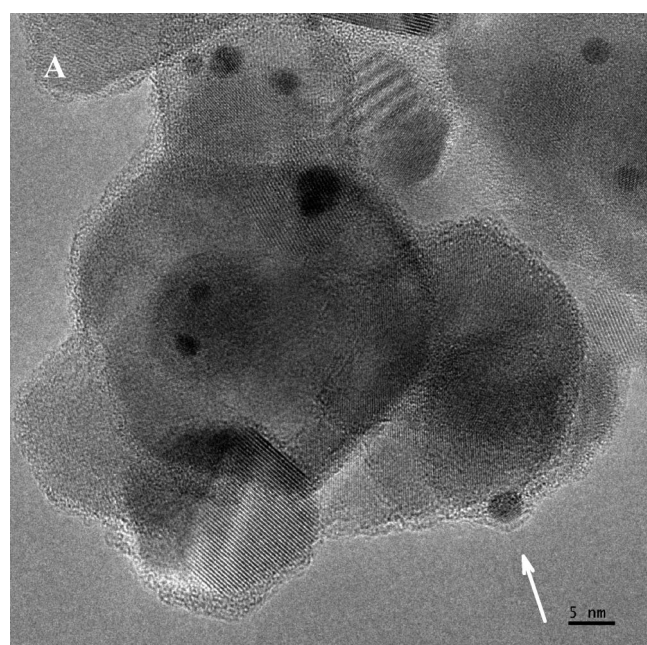


Figure 10. TEM images of used $\text{SiO}_2/\text{Au}/\text{TiO}_2$ ($\text{Si}/\text{Ti} = 0.11$) collected after pretreating the catalyst at $700\ ^\circ\text{C}$ followed by CO oxidation reported in Figure 7A.

in CO oxidation and H_2 oxidation. Overall, the net catalytic result is related to different preparation methods and preparation details. This work provides a case study on the construction of complex catalytic architectures via ALD. Although we chose the modification of gold nanocatalysts as a case study, we believe that this method can be extended to other circumstances with other active metals, supports, and coatings. The samples with advanced catalytic structures and morphologies may be useful for fundamental research on metal–support–modifier interactions and practical applications in tuning selectivity in catalysis.

Acknowledgment. This work was supported by the Office of Basic Energy Sciences, U.S. Department of Energy. The Oak Ridge National Laboratory is managed by UT-Battelle, LLC

for the U.S. DOE under Contract DE-AC05-00OR22725. This research was supported in part by the appointment for Z.M. and S.B. to the ORNL Research Associates Program, administered jointly by ORNL and the Oak Ridge Associated Universities. Dr. Hongfeng Yin assisted in the preliminary TG/DTG experiments. We thank the anonymous reviewers for providing insightful suggestions.

Supporting Information Available: TEM images of as-synthesized and 700 °C-pretreated SiO₂/Au/TiO₂ collected after the CO oxidation reaction, and a summary of the CO and H₂ oxidation conversions on Au/TiO₂ and SiO₂/Au/TiO₂ catalysts. This material is available free of charge via the Internet at <http://pubs.acs.org>.

References and Notes

- (1) Tauster, S. J. *Acc. Chem. Res.* **1987**, *20*, 389.
- (2) Baker, R. T. K.; Prestridge, E. B.; McVicker, G. M. *J. Catal.* **1984**, *89*, 422.
- (3) Singh, A. K.; Pande, N. K.; Bell, A. T. *J. Catal.* **1985**, *94*, 422.
- (4) Bernal, S.; Calvino, J. J.; Cauqui, M. A.; Gatica, J. M.; Larese, C.; Pérez Omil, J. A.; Pintado, J. M. *Catal. Today* **1999**, *50*, 175.
- (5) Bernal, S.; Calvino, J. J.; López-Cartes, C.; Pintado, J. M.; Pérez Omil, J. A.; Rodríguez-Izquierdo, J. M.; Hayek, K.; Rupprechter, G. *Catal. Today* **1999**, *52*, 29.
- (6) Rieck, J. S.; Bell, A. T. *J. Catal.* **1986**, *99*, 262.
- (7) Horváth, A.; Beck, A.; Sárkány, A.; Stefler, G.; Varga, Z.; Geszti, O.; Tóth, L.; Guczi, L. *J. Phys. Chem. B* **2006**, *110*, 15417.
- (8) Kanazawa, T. *Catal. Lett.* **2006**, *108*, 45.
- (9) Takenaka, S.; Matsumori, H.; Nakagawa, K.; Matsune, H.; Tanabe, E.; Kishida, M. *J. Phys. Chem. C* **2007**, *111*, 15133.
- (10) Tada, H.; Mitsui, T.; Kiyonaga, T.; Akita, T.; Tanaka, K. *Nat. Mater.* **2006**, *5*, 782.
- (11) Maeda, K.; Teramura, K.; Lu, D. L.; Saito, N.; Inoue, Y.; Domen, K. *Angew. Chem., Int. Ed.* **2006**, *45*, 7806.
- (12) George, S. M.; Ott, A. W.; Klaus, J. W. *J. Phys. Chem.* **1996**, *100*, 13121.
- (13) Leskelä, M.; Ritala, M. *Angew. Chem., Int. Ed.* **2003**, *42*, 5548.
- (14) Whitney, A. V.; Elam, J. W.; Zou, S. L.; Zinovev, A. V.; Stair, P. C.; Schatz, G. C.; Van Duyne, R. P. *J. Phys. Chem. B* **2005**, *109*, 20522.
- (15) Jiang, Y.-B.; Liu, N. G.; Gerung, H.; Cecchi, J. L.; Brinker, C. J. *J. Am. Chem. Soc.* **2006**, *128*, 11018.
- (16) Mahurin, S.; Bao, L. L.; Yan, W. F.; Liang, C. D.; Dai, S. *J. Non-Cryst. Solids* **2006**, *352*, 3280.
- (17) Mahurin, S. M.; Bao, L. L.; Dai, S. *Isr. J. Chem.* **2006**, *46*, 329.
- (18) Lashdaf, M.; Krause, A. O. I.; Lindblad, M.; Tiitta, M.; Venäläinen, T. *Appl. Catal., A* **2003**, *241*, 65.
- (19) Chen, C. S.; Lin, J. H.; Tou, J. H.; Chen, C. R. *J. Am. Chem. Soc.* **2006**, *128*, 15950.
- (20) Keränen, J.; Carniti, P.; Gervasini, A.; Iiskola, E. I.; Auroux, A.; Niinistö, L. *Catal. Today* **2004**, *91*–92, 67.
- (21) Pellin, M. J.; Stair, P. C.; Xiong, G.; Elam, J. W.; Birrell, J.; Curtiss, L.; George, S. M.; Han, C. Y.; Iton, L.; Kung, H.; Kung, M.; Wang, H.-H. *Catal. Lett.* **2005**, *102*, 127.
- (22) Herrera, J. E.; Kwak, J. H.; Hu, J. Z.; Wang, Y.; Peden, C. H. F. *Top. Catal.* **2006**, *39*, 245.
- (23) Stair, P. C.; Marshall, C.; Xiong, G.; Feng, H.; Pellin, M. J.; Elam, J. W.; Curtiss, L.; Iton, L.; Kung, H.; Kung, M.; Wang, H. H. *Top. Catal.* **2006**, *39*, 181.
- (24) Fan, H. J.; Knez, M.; Scholz, R.; Nielsch, K.; Pippel, E.; Hesse, D.; Zacharias, M.; Gösele, U. *Nat. Mater.* **2006**, *5*, 627.
- (25) Bond, G. C.; Thompson, D. T. *Catal. Rev.: Sci. Eng.* **1999**, *41*, 319.
- (26) Haruta, M.; Daté, M. *Appl. Catal., A* **2001**, *222*, 427.
- (27) Choudhary, T. V.; Goodman, D. W. *Top. Catal.* **2002**, *21*, 25.
- (28) Hashmi, A. S. K.; Hutchings, G. J. *Angew. Chem., Int. Ed.* **2006**, *45*, 7896.
- (29) Kung, M. C.; Davis, R. J.; Kung, H. H. *J. Phys. Chem. C* **2007**, *111*, 11767.
- (30) Bond, G. C.; Louis, C.; Thompson, D. T. *Catalysis by Gold*; Imperial College Press: London, 2006.
- (31) Dekkers, M. A. P.; Lippits, M. J.; Nieuwenhuys, B. E. *Catal. Today* **1999**, *54*, 381.
- (32) Grisel, R. J. H.; Nieuwenhuys, B. E. *Catal. Today* **2001**, *64*, 69.
- (33) Centeno, M. A.; Paulis, M.; Montes, M.; Odriozola, J. A. *Appl. Catal., A* **2002**, *234*, 65.
- (34) Mallick, K.; Surrell, M. S. *Appl. Catal., A* **2003**, *253*, 527.
- (35) Yan, W. F.; Chen, B.; Mahurin, S. M.; Hagaman, E. W.; Dai, S.; Overbury, S. H. *J. Phys. Chem. B* **2004**, *108*, 2793.
- (36) Yan, W. F.; Mahurin, S. M.; Pan, Z. W.; Overbury, S. H.; Dai, S. *J. Am. Chem. Soc.* **2005**, *127*, 10480.
- (37) Yan, W. F.; Mahurin, S. M.; Chen, B.; Overbury, S. H.; Dai, S. *J. Phys. Chem. B* **2005**, *109*, 15489.
- (38) Shou, M.; Takekawa, H.; Ju, D.-Y.; Hagiwara, T.; Lu, D.-L.; Tanaka, K. *Catal. Lett.* **2006**, *108*, 119.
- (39) Qian, K.; Huang, W. X.; Jiang, Z. Q.; Sun, H. X. *J. Catal.* **2007**, *248*, 137.
- (40) Ma, Z.; Overbury, S. H.; Dai, S. *J. Mol. Catal. A* **2007**, *273*, 186.
- (41) Zhu, H. G.; Ma, Z.; Overbury, S. H.; Dai, S. *Catal. Lett.* **2007**, *116*, 128.
- (42) Yan, W. F.; Ma, Z.; Mahurin, S. M.; Jiao, J.; Hagaman, E. W.; Overbury, S. H.; Dai, S. *Catal. Lett.* **2008**, *121*, 209.
- (43) Liu, J. In *Nanotechnology in Catalysis*; Zhou, B., Hermans, S., Somorjai, G. A., Eds.; Kluwer Academic/Plenum Publishers: New York, 2004; Vol. 2, p 361.
- (44) Baker, R. T.; Bernal, S.; Calvino, J. J.; Pérez-Omil, J. A.; López-Cartes, C. In *Nanotechnology in Catalysis*; Zhou, B., Hermans, S., Somorjai, G. A., Eds.; Kluwer Academic/Plenum Publishers: New York, 2004; Vol. 2, p 403.
- (45) Goodman, D. W. *Catal. Lett.* **2005**, *99*, 1.
- (46) Elam, J. W.; Groner, M. D.; George, S. M. *Rev. Sci. Instrum.* **2002**, *73*, 2981.
- (47) Bell, A. T. In *Catalyst Design: Progress and Perspectives*; Hegedus, L. L., Bell, A. T., Chen, N. Y., Haag, W. O., Wei, J., Aris, R., Boudart, M., Gates, B. C., Somorjai, G. A., Eds.; Wiley-Interscience: New York, 1987; p 103.
- (48) *Catalysis from A to Z: A Concise Encyclopedia*; Cornils, B., Herrmann, W. A., Schlögl, R., Wang, C.-H., Eds.; Wiley-VCH: Weinheim, Germany, 2000.
- (49) Zhu, H. G.; Ma, Z.; Clark, J. C.; Pan, Z. W.; Overbury, S. H.; Dai, S. *Appl. Catal., A* **2007**, *326*, 89.
- (50) Ma, Z.; Brown, S.; Overbury, S. H.; Dai, S. *Appl. Catal., A* **2007**, *327*, 226.
- (51) Ma, Z.; Zaera, F. *Surf. Sci. Rep.* **2006**, *61*, 229.
- (52) Ma, Z. *J. Colloid Interface Sci.* **2006**, *304*, 419.
- (53) Yu, K. M. K.; Yeung, C. M. Y.; Thompsett, D.; Tsang, S. C. *J. Phys. Chem. B* **2003**, *107*, 4515.
- (54) Kong, T. S. A.; Yu, K. M. K.; Tsang, S. C. *J. Nanosci. Nanotechnol.* **2006**, *6*, 1167.
- (55) Lee, D.; Zhang, L.; Oyama, S. T.; Niu, S.; Saraf, R. F. *J. Membr. Sci.* **2004**, *231*, 117.
- (56) Heinrichs, B.; Lambert, S.; Job, N.; Pirard, J.-P. In *Catalyst Preparation: Science and Engineering*; Regalbuto, J., Ed.; Taylor & Francis (CRC Press): Boca Raton, 2006; p 163.